RESEARCH ARTICLE

Proteome-wide changes induced by the Hsp90 inhibitor, geldanamycin in anaplastic large cell lymphoma cells

Jonathan A. Schumacher[1], David K. Crockett[1], Kojo S. J. Elenitoba-Johnson[2] and Megan S. Lim[2]

[1] Associated and Regional University Pathologists (ARUP), Institute for Clinical and Experimental Pathology, Salt Lake City, UT, USA
[2] Department of Pathology, University of Michigan Health Sciences Center, Ann Arbor, MI, USA

The molecular chaperone heat shock protein 90 (Hsp90) affects the function of many oncogenic signaling proteins including nucleophosmin-anaplastic lymphoma kinase (NPM-ALK) expressed in anaplastic large cell lymphoma (ALCL). While ALK-positive ALCL cells are sensitive to the Hsp90 inhibitor and the geldanamycin (GA) analog, 17-allylamino-17-demethoxygeldanamycin (17-AAG), the proteomic effects of these drugs on ALK-positive ALCL cells are unpublished. In this study, we investigated the cellular, biologic, and proteomic changes occurring in ALK-positive ALCL cells in response to GA treatment. GA induced G_2/M cell cycle arrest and caspase-3-mediated apoptosis. Furthermore, quantitative proteomic changes analyzed by cleavable isotope-coded affinity tag™-LC-MS/MS (cICAT™-LC-MS/MS) identified 176 differentially expressed proteins. Out of these, 49 were upregulated 1.5-fold or greater and 70 were downregulated 1.5-fold or greater in GA-treated cells. Analysis of biological functions of differentially expressed proteins revealed diverse changes, including induction of proteins involved in the 26S proteasome as well as downregulation of proteins involved in signal transduction and protein and nucleic acid metabolism. Pathway analysis revealed changes in MAPK, WNT, NF-κB, TGFβ, PPAR, and integrin signaling components. Our studies reveal some of the molecular and proteomic consequences of Hsp90 inhibition in ALK-positive ALCL cells and provide novel insights into the mechanisms of its diverse cellular effects.

Received: February 1, 2007
Revised: March 20, 2007
Accepted: April 17, 2007

Keywords:
ALCL / Geldanamycin / NPM-ALK

Correspondence: Dr. Megan S. Lim, University of Michigan, Department of Pathology, M5242 Medical Science Building 1, 1301 Catherine Road, Ann Arbor, MI 48105, USA
E-mail: meganlim@med.umich.edu
Fax: +1-734-936-2756

Abbreviations: 17-AAG, 17-allylamino-17-demethoxygeldanamycin; **ALCL,** anaplastic large cell lymphoma; **cICAT™,** cleavable isotope-coded affinity tag™; **GA,** geldanamycin; **Hsp90,** heat shock protein 90; **JAK/STAT,** janus kinase/signal transducer and activator of transcription; **MAPK,** mitogen-activated protein kinase; **NF-κB,** nuclear factor kappa B; **NPM-ALK,** nucleophosmin-anaplastic lymphoma kinase; **PPAR,** peroxisome proliferator-activated receptor; **TGFβ,** transforming growth factor β

1 Introduction

Anaplastic large cell lymphoma (ALCL) is a type of non-Hodgkin lymphoma that commonly harbors the t(2;5)(p23;q35) chromosomal aberration, resulting in the expression of the 80 kDa nucleophosmin-anaplastic lymphoma kinase (NPM-ALK) fusion oncoprotein [1–3]. Native NPM is a nucleolar phosphoprotein, whose functions include ribosomal RNA assembly, chaperone activities, and nuclease activity [4]. ALK is a 200 kDa receptor tyrosine kinase [5] belonging to the insulin receptor superfamily [6]. An N-terminal oligomerization domain within NPM facilitates the dimerization of NPM-ALK, leading to autophos-

phorylation and constitutive activation of the ALK tyrosine kinase [5]. Activated ALK induces multiple downstream signaling molecules including phospholipase Cγ (PLCγ) [7], phosphatidylinositol-3-kinase (PI3K) [8]/RAC protein kinase (AKT) [9], Janus kinase 3 (JAK3) [10], signal transducer and activator of transcription 3 (STAT3) [11], and the nonreceptor protein kinase sarcoma (SRC) [12] which leads to enhanced cell proliferation, survival, and apoptosis inhibition [13].

The benzoquinone ansamycins geldanamycin (GA) and derivative, 17-allylamino-17-demethoxygeldanamycin (17-AAG) elicit antitumor activity in a variety of cancer cell lines, including ALCL [14, 15]. Heat shock protein 90 (Hsp90) has been identified as the primary target of GA [16]. Hsp90 is a highly conserved, ubiquitous molecular chaperone that is required for the stability and conformational maturation of a diverse group of client proteins, including components of signaling pathways exploited by cancer cells for survival and proliferation [17]. Hsp90 client proteins include receptor tyrosine kinases such as human epidermal growth factor receptor (EGFR) [18] family kinases, breakpoint cluster region-Abelson (BCR-ABL), and NPM-ALK; cytosolic signaling proteins such as AKT, v-raf-1 murine leukemia viral oncogene homolog 1 (RAF-1), and inhibitor of nuclear factor kappa (IKK) as well as cell cycle regulators including cyclin-dependent kinase 4 (cdk4), polo-like kinase 1 (PLK1), and survivin [17, 19, 20]. Inhibition of Hsp90 by ansamycins in ALK-positive ALCL cells results in downregulation of NPM-ALK protein kinase activity [14] leading to cellular apoptosis [15]. Clearly, there are multiple cellular targets of Hsp90, yet the comprehensive effects of Hsp90 inhibition in ALK-positive ALCL cells are unknown.

Recent developments in multidimensional LC techniques combined with MS/MS have enabled sensitive and high-throughput detection of low abundance proteins [21]. This technology combined with a cleavable isotope-coded affinity tag (cICAT™) approach allows for the global quantitative analysis of proteins in complex mixtures [22]. In this study, we sought to assess the cellular, biologic, and quantitative proteomic changes occurring in ALK-positive ALCL cells in response to Hsp90 inhibition by GA. Our results demonstrate that GA induced G_2/M cell cycle arrest and caspase-3-mediated apoptosis. Moreover, we identified 49 proteins that were upregulated 1.5-fold or greater and 70 proteins downregulated 1.5-fold or greater in GA-treated cells. Importantly, we identified several proteins involved in diverse cellular functions, including signal transduction, DNA metabolism, nucleic acid and protein metabolism, cell growth and maintenance, and energy pathways. Some of the downregulated proteins are known to be involved in described signaling pathways such as JAK/STAT as well as pathways previously unreported in ALK-positive ALCL including mitogen-activated protein kinase (MAPK), WNT, nuclear factor kappa B (NF-κB), transforming growth factor β (TGFβ), peroxisome proliferator-activated receptor (PPAR), and integrin signaling. Our studies demonstrate some of the molecular mechanisms by which Hsp90 inhibition leads to reduced viability of ALK-positive ALCL cells and reveals cellular proteins whose expression is changed due to GA inhibition of Hsp90.

2 Materials and methods

2.1 Cell culture

The ALK-positive ALCL suspension cell line, SU-DHL-1, was obtained from the German Collection of Microorganisms and Cell Cultures (DSMZ, Braunschweig, Germany). Cells were cultured in RPMI 1640 (Life Technologies, Grand Island, NY) supplemented with 15% heat-inactivated FBS (Nova-Tech, Grand Island, NE), 25 mM HEPES (Invitrogen, Carlsbad, CA), 2 mM GlutaMAX™ (Invitrogen), and 1% antibiotic/antimycotic solution (Invitrogen) at 37°C in a humidified atmosphere of 95% oxygen and 5% CO_2.

2.2 Cell proliferation assay

Cells were seeded in 6-well plates at a density of 5×10^5 cells/mL in a final volume of 2 mL and subsequently treated with DMSO (vehicle) or concentrations of GA (A.G. Scientific, San Diego, CA) ranging from 0.032 μM through 100 μM in a volume of 10 μL. For each GA concentration, cultures were maintained in triplicate. At the end of 6-, 12-, and 24-h, 1×10^4 cells from each control and GA dose were seeded in 96-well plates in triplicate and exposed to 10 μL of WST-1 labeling solution (WST-1 cell proliferation reagent; Roche Diagnostics, Indianapolis, IN) and subsequently returned to the incubator for a period of 2 h. The rate of WST-1 cleavage by mitochondrial dehydrogenases was measured by absorbance at 450 nm using an ELISA plate reader (Molecular Devices, Sunnyvale, CA), with a reference wavelength of 600 nm.

2.3 Cell cycle analysis of DNA content

Cells (2 mL; 5×10^5 cells/mL in 6-well plates) were treated with 10 μM GA for 24 h, harvested after 6, 12, and 24 h, and prepared for cell cycle analysis as described [23]. Briefly, 1×10^5 control and GA-treated cells were fixed in 70% ethanol and stained with 0.1% sodium citrate, 200 μg/mL RNaseA, 0.5% NP-40 and 1 mg/mL propidium iodide (PI) and analyzed using an Epics XL-MCL flow cytometer (Beckman Coulter, Fullerton, CA). Cell cycle phase distribution was determined using EXPO32™ software (Beckman Coulter). Three independent experiments were performed in triplicate.

2.4 Analysis of apoptosis

Cells (2 mL; 5×10^5 cells/mL in 6-well plates) were treated with 10 μM GA for 24 h, harvested after 6, 12, and 24 h, and prepared for flow cytometric analysis as described [24].

Briefly, 1×10^6 control and GA-treated cells were stained with 10 μL annexin V-FITC (Miltenyi Biotechnology, Auburn, CA) and 10 μL PI (Miltenyi Biotechnology) and analyzed on an Epics XL-MCL flow cytometer. Three independent experiments were performed in triplicate.

2.5 Caspase-3 activity assay

Cells (2 mL; 5×10^5 cells/mL in 6-well plates) were treated with 10 μM GA for 24 h. Caspase-3 protease activity was assessed using the colorimetric Caspase-Glo™ 3/7 colorimetric assay (Promega, Madison, WI) following the manufacturer's protocol. Briefly, 1×10^4 cells were harvested after 6, 12, and 24 h, seeded in 96-well white-walled plates, and incubated with 100 μL of caspase-3 substrate, Ac-DEVD-aminoluciferin. After ambient incubation in the dark for 1 h, the release of aminoluciferin was measured on a luminometer (ThermoLabsystems, Waltham, MA). Readings for blank control was subtracted from experimental readings. Furthermore, cells were treated with 100 μM caspase-3 inhibitor, Z-DEVD-FMK (EMD Biosciences, San Diego) for 15 min followed by 10 μM GA and assay repeated. Three independent experiments were performed in triplicate.

2.6 Protein isolation and immunoprecipitation

Briefly, cells were collected by centrifugation and washed twice in PBS. Whole cell lysates were prepared using 500 μL RIPA lysis buffer (1% NP-40, 0.1% SDS, 0.5% DOC, 20 mM Tris (pH 7.5), 100 mM NaCl, 0.2% protease inhibitor, and 2 mM activated sodium orthovanadate). After 30-min incubation on ice, samples were centrifuged at 14 000 rpm for 15 min at 4°C. Supernatants were recovered and protein concentrations determined using the Bradford colorimetric assay with BSA standards (Pierce Chemical, Rockford, IL).

2.7 Immunoblot analysis

For immunoblot analysis, 25 μg of lysate from control and GA-treated cells were mixed with 10 μL of Laemmli reducing buffer and heated at 95°C for 5 min. Samples were subsequently resolved by SDS-PAGE on 4–12% gel and electrophoretically transferred to PVDF membranes. Membranes were blocked for 1 h in blocking solution (5% nonfat milk diluted in TBS (20 mM Tris-HCl, pH 7.4, 150 mM NaCl, and 0.1% Tween-20)). The following antibodies were used for immunoblot analysis: mouse polyclonal antibodies against PARP, p21, and p27; goat polyclonal antibodies against ras GTPase-activating protein 3 (RARS3), paracellin-1 (PCLN1), and stanniocalcin-1 (STCN1); and rabbit polyclonal antibody against actin from Santa Cruz Biotechnology (Santa Cruz, CA); mouse polyclonal antibodies against Hsp90 and NEMO (Becton Dickinson Pharmingen, San Diego); rabbit polyclonal antibodies against phospho-ALK and ALK (Cell Signaling, Beverly, MA); rabbit polyclonal antibody against ubiquitin-specific protease 9 (USP9) (Abgent, San Diego); mouse polyclonal antibodies against tankyrase (TNKS) and osteoprotegerin (OPG) and rabbit polyclonal antibodies against suppressor of cytokine signaling 4 (SOCS4; Acris Antibodies, Hiddenhausen, Germany). Membranes were incubated from 1 h at room temperature to 4°C overnight with primary antibodies in TBST containing 3% nonfat dry milk, washed five times with TBST, and probed with HRP-labeled secondary antibody at room temperature for 1 h. After five washes with TBST, immunoreactive bands were visualized by chemiluminescence (Amersham Biosciences, Piscataway, NJ). Densitometry was performed using Image J software (National Institutes of Health (NIH), Bethesda, MD) and values were normalized to actin controls.

2.8 cICAT labeling of proteins and 3-D LC-MS/MS

SU-DHL-1 control and cells exposed to 10 μM GA were harvested after 12 h incubation and prepared for analysis of differential protein expression as described in ref. [25] (see Fig. 1 for illustration). Briefly, 400 μg of protein from both samples were reduced with 2.5 mM Tris (2-carboxyethyl) phosphine (Sigma) for 1-h at 37°C. Isotope labeling was performed by mixing 1 U of light (control sample) or heavy (GA-treated sample) cleavable cICAT reagent with protein samples, following manufacturer's protocol (Applied Biosystems). Labeled proteins from control and treated samples were mixed and dialyzed against 500 mL of urea buffer (2 M urea, 10 mM Tris, pH 8.5) three times for 1-h each at room temperature using a 3.5 kDa cutoff dialysis cassette (Pierce). The dialyzed protein mixtures were then diluted two-fold with 10 mM Tris, pH 8.5, before digestion with 10 μg of modified trypsin (Promega) overnight at 37°C. The peptide mixture was then acidified to pH$\leq$3.0 by adding TFA before loading onto the cation exchange column. The 3-D liquid chromatographic separation of peptides was performed by first, strong cation-exchange (SCX) chromatography using a 3.6 mm × 20 cm polysulfoethyl A column (Poly LC, Columbia, MD) at a flow rate of 400 μL/min with 35 fractions collected (800 μL/fraction). A two-step linear buffer gradient was used: 5% buffer B and 95% buffer A to 25% buffer B and 75% buffer A for 50 min followed by 25% buffer B and 75% buffer A to 100% buffer B for 18 min (buffer A: 20 mM KH_2PO_4, 25% ACN pH 3.0; buffer B 350 mM KCL in buffer A pH 3.0). Next, 35 fractions collected from the offline SCX chromatography were further washed and purified by avidin affinity chromatography (Applied Biosystems) to enrich for cysteine containing (cICAT-labeled) peptides followed by drying and cleaving of eluted peptides. Finally, a 15 μL aliquot of each sample was analyzed by automated nanoflow RP LC/MS using the LCQ Deca XP IT mass spectrometer (Thermo-Finnigan, San Jose, CA). Digested peptides were injected by an autosampler, using an ACN gradient (0–60% B in 120 min; A = 5% ACN with 0.4% acetic acid and 0.005% HFBA) through a RP column (75 μm id fused silica packed in-house with 10 cm of 5 μm C18 particles) to elute the peptides at a flow rate of ~200 nL/min into the mass spectrom-

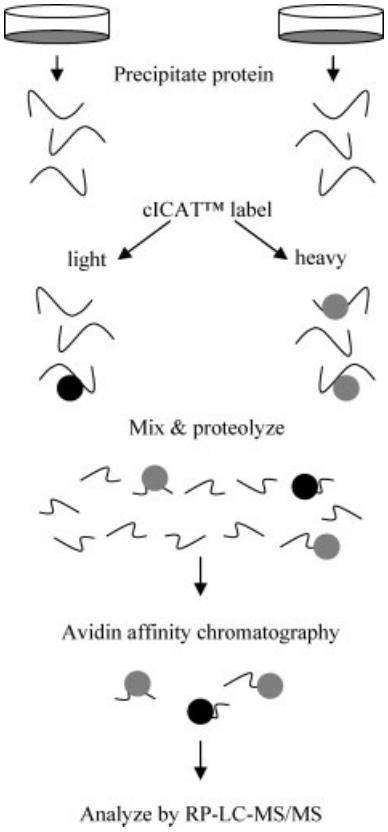

Figure 1. cICAT strategy to isolate and identify differentially expressed proteins in GA-treated cells relative to control. Cells were in the presence of 1% DMSO (control) or 10 μM GA for 12 h. Total cellular protein was precipitated under reduced conditions. Total protein from control cells was labeled with the light cICAT reagent (black circle) and protein from GA-treated cells labeled with the heavy cICAT reagent (gray circles). Samples were mixed, proteolyzed in trypsin, and subjected to avidin affinity chromatography. Isolated cICAT-labeled peptides were subjected to LC-MS/MS to quantitate and identify differentially expressed proteins.

eter. An electrospray voltage of 1.8 kV was used with the ion transfer tube temperature set to 200°C. Peptide analysis was performed using data-dependent acquisition of one MS scan (600–2000 m/z) followed by MS/MS scans of cICAT peptide pairs triggered by the isotope tag mass difference of 9.0 amu. To obtain better peptide coverage, dynamic exclusion was set to a repeat count of 3, with the exclusion duration of 5 min.

2.9 Data analyses

The MS/MS acquired data were searched using the SEQUEST algorithm in Bioworks 3.1 (ThermoFinnigan) against human amino acid sequences in the 9.23.2004 download of the NCBI nr.fasta protein database with 191 136 entries. Protein search parameters included a precursor peptide mass tolerance of ± 0.7 amu and fragment mass tolerance of ± 0.1 amu. To account for the isotope label, static modification of cysteine was set to 227.13 and differential modification of cysteine set as 9.0. The search was constrained to tryptic peptides with one missed enzyme cleavage allowed. The peptide matching criteria of a cross correlation score (X_{corr})>1.2 for +1 peptides, >2.2 for +2 peptides, and >3.2 for +3 peptides, and a delta correlation score (ΔC_n)>0.100 was used as a threshold of acceptance. cICAT protein quantification was performed using XPRESS™ software (Thermo) which automatically calculates the relative abundance of light and heavy cICAT-labeled peptide as a ratio of light database containing both forward and reverse amino acid sequences for each protein entry. The total number of proteins identified with reverse sequence entries is then multiplied (2 ×) to compensate for doubling the size of the database. Overall, the predicted false positive rate for protein identification by LC-MS/MS was 7.1%.

Differentially expressed proteins were further analyzed using the Ingenuity™ Pathways Analysis (Ingenuity, Mountain View, CA) web-based application software tool and Bioinformatics Harvester database. Protein accession numbers and corresponding cICAT expression values were saved into the Ingenuity Systems template.xls file. Files were submitted on-line for analysis and comparison to the Ingenuity gene/protein interaction knowledge base (http://www.ingenuity.com/). The results for the pathways and protein interactions were summarized and interaction network images generated with respect to putative canonical pathways. Individual proteins were submitted to the Bioinformatics Harvester database (http://harvester.embl.de/) and protein functional characteristics analyzed.

3 Results

3.1 GA reduces cell viability

In order to establish the proteome-wide changes induced by GA in ALK-positive ALCL cells, we first sought to assess the effects of GA on cell viability.

Previous studies have demonstrated that ansamycins target Hsp90 and inhibit its function as a molecular chaperone. To determine if GA induced similar effects on ALK-positive ALCL cells, we cultured the NPM-ALK-positive ALCL cell line, SU-DHL-1, with increasing concentrations of GA up to 24 h and measured cell viability using the WST-1 assay. As shown in Fig. 2A, the most effective drug concentration was between 4 and 20 μM, with IC_{50} values of 10.9, 13.3, and 13.6 μM at 6, 12, and 24 h, respectively. There was no statistically significant reduction in viability between 20 and 100 μM demonstrating the maximum effects of the drug. We subsequently treated SU-DHL-1, Karpas299, and DEL cells in the presence or absence of 10 μM GA and measured cell viability at 6, 12, and 24 h. Figure 2B illustrates the effects of GA on cell viability in a time-dependent manner. Based on our preliminary dose-dependence results, we selected a concentration of 10 μM for subsequent experiments.

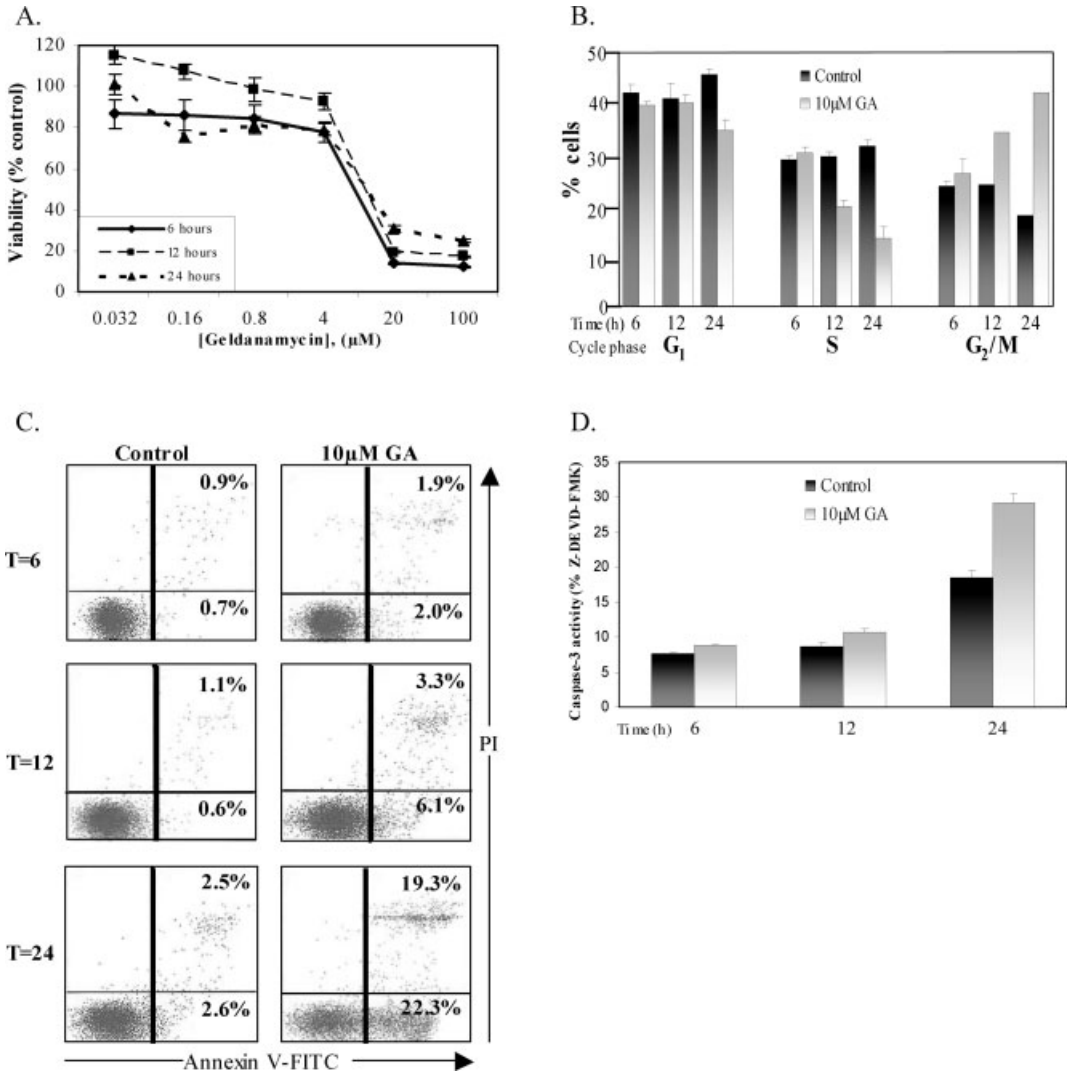

Figure 2. (A) GA reduces cell viability. Cells were cultured in the presence of 1% DMSO or various concentrations of GA for the indicated times and cell viability assessed by WST-1 reduction assay. Concentrations of GA are listed on the *x*-axis. Viability as percent of control is listed on the *y*-axis. Results are expressed as the mean of three independent experiments performed in triplicate ± SDs. Data are normalized to DMSO control. (B) GA induces G_2/M cell cycle arrest. Control and GA-treated cells were harvested and fixed after 6, 12, and 24 h incubation. Cellular DNA content was determined by flow cytometric analysis after RNase treatment and PI staining. Time and DNA content are denoted on the *x*-axis and % cells are denoted on the *y*-axis. Results are expressed as the mean of three independent experiments, performed in triplicate ± SDs. (C) GA induces apoptosis. Control and GA-treated cells were harvested after 6, 12, and 24 h and stained with annexin V-FITC/PI. Cellular apoptosis was determined by flow cytometric analysis. Annexin V-FITC staining is denoted on the *x*-axis. PI staining is denoted on the *y*-axis. Left panels illustrate the staining patterns of control for each time point. Right panels illustrate the staining patterns of GA-treated cells for the same time points. The percent of cells in each particular quadrant represents the mean of three independent experiments. SDs were within 5% of the mean. (D) GA-induced apoptosis is mediated by caspase-3. Control and GA-treated cells were harvested after 6, 12, and 24 h. Caspase-3 activity was determined by luminescence detection of caspase-3 substrate cleavage. Time is denoted on the *x*-axis. The increase in caspase-3 luminescence as a percent of Z-DEVD-FMK control is denoted on the *y*-axis. Results are expressed as the mean values of three independent experiments, performed in triplicate ± SDs.

3.2 GA induces G_2/M cell cycle arrest

We investigated the effects of GA on cell cycle phase distribution to determine whether cell viability reduction was caused by disruption of cell cycle-related events. Cells cultured in 10 μM GA were harvested at the indicated times, stained with PI, and subjected to cell cycle analysis. The percent of cells in G_1 were unchanged at 6 and 12 h, but were reduced by 10.8% after 24 h, relative to control (Fig. 2C). A reduction of cells in S-phase was seen at 12 and 24 h by 9.9 and 18%, respectively, compared to control. In contrast, cells in G_2/M increased by 10.4 and 24.2% after 12

and 24 h, compared to control. These data suggest that the reduction of cell viability is due to a block in the G_2/M transition.

3.3 GA induces caspase-3-mediated apoptosis

To further analyze the effects of GA on cell viability, we performed time-course flow cytometric analysis of annexin V-FITC/PI stained cells. Figure 2D illustrates the time-dependent increase in apoptotic cells in response to GA after 6, 12, and 24 h. The fraction of early and late apoptotic cells (annexin V-positive/PI negative and annexin V-positive/PI-positive) increased by 2.3% at 6 h, 7.7% at 12 h, and 36.5% at 24 h, respectively, relative to control. To evaluate the mechanism of GA-induced apoptosis, we analyzed caspase-3 activity. As shown in Fig. 2E, GA induced a time-dependent increase in caspase-3 activity by 1.3, 2.0, and 10.7% at 6, 12, and 24 h, respectively, relative to control. Furthermore, caspase-3 activity was completely inhibited by the caspase-3 inhibitor Z-DEVD-FMK at all time points. These results demonstrate that GA induces caspase-3-mediated apoptosis.

3.4 Effects of GA on NPM-ALK, Hsp90, cell cycle regulatory proteins, and apoptosis regulatory proteins

To examine the underlying mechanisms by which GA arrested cells in G_2/M and induced caspase-3-mediated apoptosis, we performed immunoblot analysis to determine relative expression of phosphorylated and nonphosphorylated NPM-ALK, Hsp90, $p21^{CIP1}$, $p27^{KIP1}$, and PARP. After 12 h drug treatment, the expression of both nonphosphorylated and phosphorylated NPM-ALK expression was markedly reduced in GA-treated cells (Fig. 3). In contrast, expression of Hsp90 remained unchanged. While expression of the Cdk2 inhibitor, $p21^{CIP1}$ was unchanged, the expression of the Cdk4 inhibitor, $p27^{KIP1}$ was induced in GA-treated cells. Moreover, PARP underwent cleavage into its 85 kDa fragment with GA treatment, consistent with apoptosis. The levels of actin remained unchanged.

3.5 MS/MS analysis of cICAT-labeled peptides

We sought to survey the proteomic changes induced by GA inhibition of Hsp90 using cICAT- LC-MS/MS. Top protein database search hits from SEQUEST were summarized using BioWorks 3.1 and the relative quantification calculated using XPRESS. Figure 4 displays an example of the MS-full scan and MS/MS scan for the cICAT-labeled peptide sequence corresponding to SOCS4. Examination of the data from 35 individual SCX fractions resulted in a total of 2921 peptides identified, which were matched to 1129 known NCBI database entries and 314 unique proteins. Of the 176 cICAT-labeled peptides, 119 were differentially expressed by 1.5-fold or greater at 12 h. Over- and underexpressed proteins

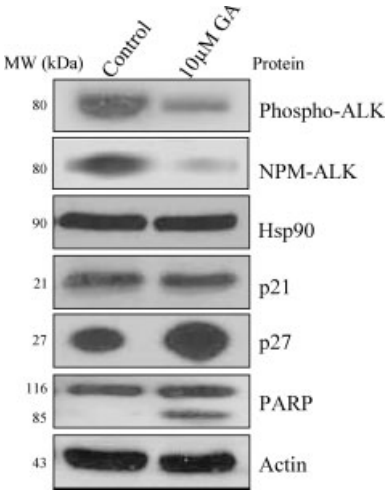

Figure 3. GA inhibition of Hsp90 influences expression of a variety of proteins. Total cell lysate was extracted from control and GA-treated cells after 12 h and proteins separated by SDS-PAGE. Immunoblots were probed with antiphospho-ALK (1:1000), anti-NPM-ALK (1:1000), anti-Hsp90 (1:1500), anti-p21 (1:500), anti-p27 (1:500), anti-PARP (1:1500), and antiactin (1:500); incubated at room temperature for 1 h (Hsp90, p21, p27, PARP, and actin) or overnight at 4°C (phospho-ALK and NPM-ALK), followed by probing with respective horseradish-peroxidase conjugated secondary antibodies and visualized by chemiluminescence. Actin served as a loading control. Protein sizes are listed left of each immunoblot.

were categorized by biological process (Table 1). A large number of the differentially expressed proteins were down-regulated (59%) in response to GA.

The Bioinformatics Harvester database (http://harvester.embl.de/) was used to perform analysis of protein functional characteristics using the 1.5-fold threshold. Seventy-seven percent of the proteins identified and quantified have known functions, while 23% were assigned to the hypothetical category. Furthermore, 84% of the identified proteins were assigned to nuclear, cytoplasmic, membranous, or extracellular locations while the subcellular locations of the remaining 16% are unknown. Figure 5A illustrates localization of overexpressed proteins and Fig. 5B illustrates localization of underexpressed proteins in GA-treated cells. Analysis of localization demonstrated the majority of proteins exist in the nucleus and cytoplasm (67% of overexpressed and 75% of underexpressed).

Analysis of biological pathways of differentially expressed proteins using the Ingenuity Pathways Analysis tool revealed deregulated proteins involved in a variety of pathways, including integrin, estrogen receptor, MAPK, JAK/STAT, PPAR, and NF-κB signaling as well as those involved in ubiquitin-mediated proteolysis and cell cycle regulation. Several of the proteins are involved in multiple functions such as the *versus* heavy [25].

The false-positive error rate for protein identifications was calculated using the composite target/decoy database method [26]. Acquired MS/MS spectra were searched against

Table 1. Differentially expressed proteins of 1.5-fold over- and underexpressed, categorized by biological function

	Name	Description	NCBI	Fold	Peptides	X_{corr}	Charge state
Cell signaling							
Overexpressed	MAP4K1	Mitogen-activated protein kinase kinase kinase kinase 1	6005810	25.0	-.SSSLGIPDADC*CR.-	1.38	1
	WNT10B	Wingless-type MMTV integration site family, member 10B precursor	16936522	8.3	-.C*HGTSGSCQFK.-	2.58	2
	CLK2	Dual specificity protein kinase CLK2 (CDC-like kinase 2)	1705919	3.6	-.VVQC*VDHRRGGAR.-	2.62	2
	RASA3	Ras GTPase-activating protein 3 (GAP1(IP4BP))	13959562	2.8	-.ALYIQANNC*VEAK.-	2.53	2
	PLEKHA2	Pleckstrin homology domain-containing protein family A member 2	48474645	2.4	-.TPFC*FVINALSQR.-	2.54	2
	RAPGEF6	Rap guanine nucleotide exchange factor 6	34395686	2.3	-.LLNIAC*AAKAKWR.-	2.52	2
	MAPK14	Mitogen-activated protein kinase kinase kinase 14	4505397	2.2	-.LISPLQC*LNHVWK.-	1.23	1
	STC1	Stanniocalcin 1	4507265	2.1	-.ESLKC*IANGVTSK.-	2.12	1
	IL1R1	Interleukin-1 receptor, type I precursor	4504659	1.9	-.QC*GYKLFIYGR.-	2.05	1
	ARHGAP20	Rho GTPase-activating protein 20	25535895	1.8	-.VSLLIQFLIENC*LR.-	1.48	1
	SMAD5	SMAD, mothers against DPP homolog 5; Dwfc	47778925	1.8	-.PLDIC*EFPFGSK.-	2.65	2
Underexpressed	GRIN2D	*N*-methyl-D-aspartate receptor subunit 2-D precursor; estrogen receptor	4504131	7.1	-.CC*KGFC*IDILKR.-	3.00	2
	IL26	Interleukin 26 precursor	8923756	7.1	-.C*GLLLVTLSLAIAK.-	2.59	2
	ZP4	Zona pellucida glycoprotein 4 preproprotein; zona pellucida B protein	10863987	7.1	-.KLLKC*PMDLLAR.-	2.55	2
	PTK2B	Protein tyrosine kinase 2 β isoform a; (PTK2B) cell adhesion kinase	27886584	6.7	-.PTC*LAEFKQIRSIR.-	1.45	1
	PI-G PLD	Similar to phosphatidylinositol-glycan-specific	28828281	5.6	-.C*NAILYAGAMGVK.-	1.60	1
	STIP1**	Stress-induced-phospho-protein 1 (Hsp70/Hsp90-organizing protein)	5803181	5.0	-.ELC*EKAIEVGRENR.-	1.38	1
	PDC	Phosducin isoform a; G β γ binding protein	32967591	4.6	-.FC*KIKASNTGAGDR.-	2.62	2
	RAD17	Checkpoint protein, involved in the activation of the DNA damage	6324944	4.0	-.DYPGIVIEVC*MLEK.-	2.56	2
	CBLC	Signal transduction protein CBL-C (SH3-binding protein CBL-C)	46397888	3.6	-.APAHTFWRESC*GAR.-	2.58	2
	GRB7	Growth factor receptor-bound protein 7	4885355	2.5	-.PHVVKVYSEDGAC*R.-	1.38	1
	RPS6KB1	Ribosomal protein S6 kinase, 70 kDa, polypeptide 1	4506737	2.5	-.IRPEC*FELLRVLGK.-	2.19	1
	SOCS4	Suppressor of cytokine signaling 4 (SOCS4)	20178095	2.4	-.PTNSEETC*IKMEVR.-	1.90	1
	ANAPC4	Anaphase promoting complex subunit 4 (APC4)	37537862	2.4	-.SMNQAIC*IPLYR.-	2.79	2

Table 1. Continued

	Name	Description	NCBI	Fold	Peptides	X_{corr}	Charge state
	IKBKG**	Inhibitor of kappa light polypeptide gene enhancer in B-cells (NEMO)	4504631	2.4	-.C*QQQMAEDKASVK.-	2.54	2
	T3JAM	TRAF3-interacting JNK-activating modulator	13435127	2.2	-.C*RPNVTTCRQVGK.-	1.40	1
	MAK**	Male germ cell-associated kinase	11496279	2.1	-.KFYSWDEC*MNLR.-	2.52	2
	PDE5A	Phosphodiesterase 5A isoform 1; cGMP-binding cGMP-specific	4505667	2.0	-.VHTIPVC*KEGIR.-	1.31	1
	RAC3	Ras-related C3 botulinum toxin substrate 3	4826962	2.0	-.HHC*PHTPILLVGTK.-	1.41	1
	TNFRSF11B	Human osteoprotegerin (OPG) protein	2072185	1.8	-.VGAEDIEKTIKAC*K.-	1.57	1
	DKK2	Dickkopf homolog 2; Dickkopf gene 2	7657023	1.7	-.GKNLGQAYPC*SSDK.-	2.63	2
	+	Myelin oligodendrocyte glycoprotein isoform 2	45580732	1.6	-.FSDEGGFTC*FFR.-	2.58	2
DNA metabolism							
Overexpressed	ZNF297	Zinc finger protein 297 (BING1 protein)	23396973	9.1	-.PFDCPVC*NKKFK.-	1.34	1
	CTCF	CCCTC-binding factor (zinc finger protein)	5729790	2.6	-.PHKC*HLCGRAFR.-	2.11	1
	OIP106	106 kDa O-GlcNAc transferase-interacting protein	13124654	1.7	-.YFLLC*AERVGQMTK.-	1.29	1
	THOC1	Nuclear matrix protein p84	4826882	1.7	-.QIEC*DSEDMKMRAK.-	2.13	1
Underexpressed	GTBP	GTBP-N protein	7512474	6.7	-.GLSFPRRGC*GLER.-	2.80	2
	TNKS	Tankyrase, TRF1-interacting ankyrin-related ADP-ribose polymerase	4507613	4.2	-.ELLEAC*RNGDVSR.-	2.78	2
	HILS1	Spermatid-specific linker histone H1-like protein	34850057	4.0	-.GTC*KYVSLATLKK.-	2.52	2
	+	Similar to cofactor required for Sp1 transcriptional activation	38086032	3.9	-.TDALKC*RVALSPK.-	1.51	1
	ZNF324	Zinc finger protein 324 (*Homo sapiens*)	7657693	3.1	-.PFRCVDC*GKAFAK.-	2.00	1
	SNRP70	U1 small nuclear ribonucleo-protein 70 kDa	29568103	3.0	-.HHNQPYC*GIAPYIR.-	1.28	1
	SRrp35	35 kDa SR repressor protein (SRrp35)	47606193	2.8	-.HSDSIARSPC*KSPK.-	2.50	2
	ZNF516	Zinc finger protein 516	14548318	2.7	-.GSFDHGC*HICGRR.-	1.43	1
	SIX5	Homeobox protein SIX5	46396941	2.5	-.AC*YRGNRYPTPDEK.-	1.85	1
	JRK	Jerky protein homolog	27805484	2.1	-.QPC*FSAQEVGQLR.-	2.57	2
	POLRD3	RNA polymerase III 53 kDa subunit RPC4	4502437	1.9	-.LVC*SPDFESLLDHK.-	1.68	1
Protein metabolism							
Overexpressed	PSMD9	26S proteasome non-ATPase regulatory subunit 9	12230943	5.6	-.GLLGC*NIIPLQR.-	2.65	2
	USP9X	Ubiquitin specific protease 9	11641423	5.6	-.WYKFDDGDVTEC*K.-	1.56	1
	ADAMTS12	A disintegrin-like and metall-oprotease	13569928	4.4	-.ATFC*DPETQPNGR.-	2.55	5
	AARS	Alanyl-tRNA synthetase	4501841	3.7	-.AVYTQDC*PLAAAK.-	2.01	1
	PSMD7	26S proteasome regulatory chain, p40	1085272	2.1	-.YC*PNSVLVIIDVK.-	2.59	5

Table 1. Continued

	Name	Description	NCBI	Fold	Peptides	X_{corr}	Charge state
Underexpressed	MRPS15	Mitochondrial ribosomal protein S15; 28S ribosomal protein S15	16554611	2.7	-.KALC*IRVFQETQK.-	1.69	1
	PSMD2	Proteasome β 2 subunit; proteasome subunit, beta-type, 2	4506195	2.7	-.AVELLRKC*LEELQK.-	1.80	1
	CAPN5	Calpain 5	37577157	2.2	-.NEFWC*ALVEKAYAK.-	2.07	1
	SACS	Sacsin	13124523	2.0	-.VCQFGALC*SLQGR.-	1.62	1
	PRSS15	Endopeptidase La homolog (EC 3.4.21.-) precursor	1362755	2.0	-.AGVTC*IVLPAENKK.-	2.55	2
	VCIP135	Valosin-containing protein (p97)	36029914	1.8	-.PICC*AWSSSGR.-	2.54	2
Cell growth							
Overexpressed	PCLN1	Claudin 16; paracellin-1	5729970	2.6	-.RPVFSHC*QVPETQK.-	1.35	1
	DRP2	Dystrophin-related protein 2	4503393	2.6	-.HFVPSAGADSETHC*.-	2.66	2
	AKAP6	A-kinase anchor protein 6	13431309	1.8	-.TLTC*EENLLNLHEK.-	1.85	1
	SYNE2	Nesprin 2 (Nuclear envelope spectrin repeat protein 2)	29839588	1.7	-.PVVYDVC*DDQEIQK.-	1.21	1
	CRYBA4	Crystallin, beta A4	4503059	1.7	-.MTLQC*TKSAGPWK.-	1.38	1
	LZTS1	Leucine zipper, putative tumor suppressor 1	10440566	1.5	-.GLELEVC*ENELQRK.-	1.87	1
Underexpressed	MCPH1**	Estrogen receptor beta	7441774	5.3	-.CYEVGMVKC*GSR.-	1.66	1
	XRCC4	X-ray repair cross complementing protein 4 isoform 2	12408647	2.0	-.C*VSAKEALETDLYK.-	2.12	1
	MAP1A	Microtubule-associated protein 1A (proliferation-related)	19861596	1.6	-.PCC*YIFPGGR.-	2.06	1
	DNAH9	Ciliary dynein heavy chain 9	12643822	1.5	-.LNWPHMIC*EDVRR.-	1.96	1
	TFF2	Trefoil factor 2 precursor; spasmolytic protein 1; spasmolysin	4885629	1.5	-.QESDQC*VMEVSDRR.-	3.12	2
Metabolism							
Overexpressed	AKAT1	Acetyl-Coenzyme A acetyltransferase 1 precursor	4557237	5.3	-.IHMGSC*AENTAKK.-	2.68	2
	SKD3	Suppressor of potassium transport defect 3	13540606	2.9	-.FDTKC*LAAATWGR.-	2.70	2
	PDE6C	Cone cGMP-specific 3′,5′-cyclic phosphodiesterase alpha′-subunit	1705960	2.6	-.LNVDVIDDC*EEK.-	2.50	2
	FTCD	Formiminotransferase cyclodeaminase	11140815	2.3	-.MGALDVC*PFIPVR.-	2.53	1
	+	Glycosylphosphatidylinositol 1 homolog	31981380	1.7	-.SKLSTC*EQLHHRLK.-	2.18	2
	BCHE	Butyrylcholinesterase precursor	4557351	1.6	-.LTGC*SRENETEIIK.-	2.54	2
Underexpressed	UQCRH	Ubiquinol-cytochrome c reductase hinge protein	5174745	4.6	-.ERLELC*DERDSSR.-	2.69	2
	ACACB	Acetyl-CoA carboxylase (EC 6.4.1.2)	542750	2.7	-.YRITIGNKTC*VFEK.-	1.31	1
Transport							
Overexpressed	STX17	Syntaxin 17	8923604	3.5	-.LTSSC*PDLPSQTDK.-	2.57	2
	SCN1A	Sodium channel protein type I alpha subunit	12644229	3.3	-.DSC*MSNHTAEIGK.-	2.53	2
	CACNA1H	Voltage-dependent T-type calcium channel alpha-1H subunit	23503045	2.2	-.DNGMQKC*SHIPGRR.-	1.22	1

Table 1. Continued

	Name	Description	NCBI	Fold	Peptides	X_{corr}	Charge state
Underexpressed	ADFP	Adipose differentiation-related protein; adipophilin	34577059	1.9	-.LEPQIAVANTYAC*K.-	2.77	2
Immune response							
Overexpressed	TNFRSF6B	Helicase-like protein NHL isoform 2	14790174	3.3	-.NTSYRPKVC*VLGSR.-	2.71	2
	HLA-B	HLA-B protein	2118848	2.2	-.MYGC*DLGPDGRFLR.-	1.81	1
Hypothetical							
Overexpressed	SFRS14	KIAA0365	7512968	10.0	-.AWLVSSGC*PLQVK.-	2.60	2
	+	SI:zC237L4.5 novel protein similar to human procollagen	33468666	7.1	-.PHVDEHQFC*GGK.-	2.04	1
	+	DKFZp762E1312.1	11283475	5.0	-.C*LPKSDSSSSLPK.-	1.87	1
	+	DKFZp434L243.1	7512652	4.4	-.PPGGHSNLAC*ALKK.-	2.52	2
	TRIM14	Tripartite motif protein TRIM14 isoform alpha	15208663	4.2		2.51	2
	TTC4	Tetratricopeptide repeat domain 4	39652618	3.9	-.AIIRGALC*HLELK.-	2.63	2
	SOSTDC1	DKFZp564D206.1	7512729	3.3	-.SSQEWRC*VNDK.-	2.07	1
	DLG7	KIAA0008	3183208	3.2	-.NVETKPDKGISC*K.-	1.55	2
	+	KIAA0590	7513032	2.1	-.RPLRDFVGLEDC*DK.-	2.13	1
Underexpressed	GTF2H4	XP_378195	42657571	20.0	-.LYGHPATC*LAVFR.-	2.63	2
	WDR17	WD-repeat protein 17	47606182	4.4	-.EGILC*SGSDDGTVR.-	2.51	2
	+	DKFZp434M183.1	7512659	4.0	-.DVVC*TCSLKNWR.-	2.15	1
	FGL2	Fibrinogen-like 2; fibrinogen-like protein 2; fibroleukin	5730075	2.9	-.DVC*PVRLESRGK.-	2.08	1
	+	19.0 kDa early protein	139989	2.6	-.ITKNTFSTASC*GK.-	1.82	1
	HERPUD1	Homocysteine-inducible, ER stress-inducible	7661870	2.5	-.AC*YRGNRYPTPDEK.-	1.28	1
	+	Leucine-rich repeat LGI family, member 4	21281673	2.3	-.PEEELPAASVVSC*K.-	1.60	1
	+	KIAA0232	30923325	2.3	-.PVC*LQEIMTVWNK.-	1.26	1
	+	SI:zC255F14.1 (novel protein similar to human RIM binding protein)	33468681	2.2	-.PPC*WSSSSSRQTTK.-	1.66	1
	PGLYRP4	Peptidoglycan recognition protein I-beta precursor	38604973	1.9	-.TSLKKAC*PGVVPR.-	1.79	1
	+	Interleukin-14 precursor	627504	1.9	-.PARLC*LGTPFLRSR.-	2.50	2
	ANKMY1	Ankyrin repeat and MYND domain containing protein 1	30912747	1.9	-.ESQWDPTWLYLC*K.-	1.95	1
	HES1	Human HES1 protein	5031691	1.9	-.NLSTFAVDGKDC*K.-	2.79	2
	KIAA1199	KIAA1199 protein	38638698	1.6	-.FAFC*SMKGCERIK.-	1.40	1
	INFA5	Interferon alpha-G	87983	1.6	-.MC*DLPQTHSLSNRR.-	2.14	1
	EGFL3	Multiple EGF-like domain protein 3	46395624	1.5	-.CVC*HAGYELGADGR.-	1.30	1
	SDF2	Stromal cell-derived factor 2 precursor (SDF-2)	21542241	1.5	-.C*GQPIRLTHVNTGR.-	1.84	1
	C7orf28A	DKFZp586I1023.1	7512900	1.5	-.KLC*ATQFNNIFFLD.-	2.01	1
	+	DKFZp434K1772.1	7512635	1.5	-.C*PPQLRPSR.-	2.58	2

Cells were in the presence of 1% DMSO (control) or 10 μM GA for 12 h and total cellular protein precipitated. Samples were cICAT labeled and analyzed by LC-MS/MS. Identified peptides of 1.5-fold over- and underexpressed were searched against the Bioinformatics Harvester database for biological function. Proteins were categorized by biological function (over- or underexpressed) and listed are protein names, description, NCBI GI number, fold change, identified peptides, crosscorrelation score, and charge state.
Known Hsp90 clients or interacting proteins are designated **, cICAT labeled cysteines are designated *, and unnamed proteins are designated +.

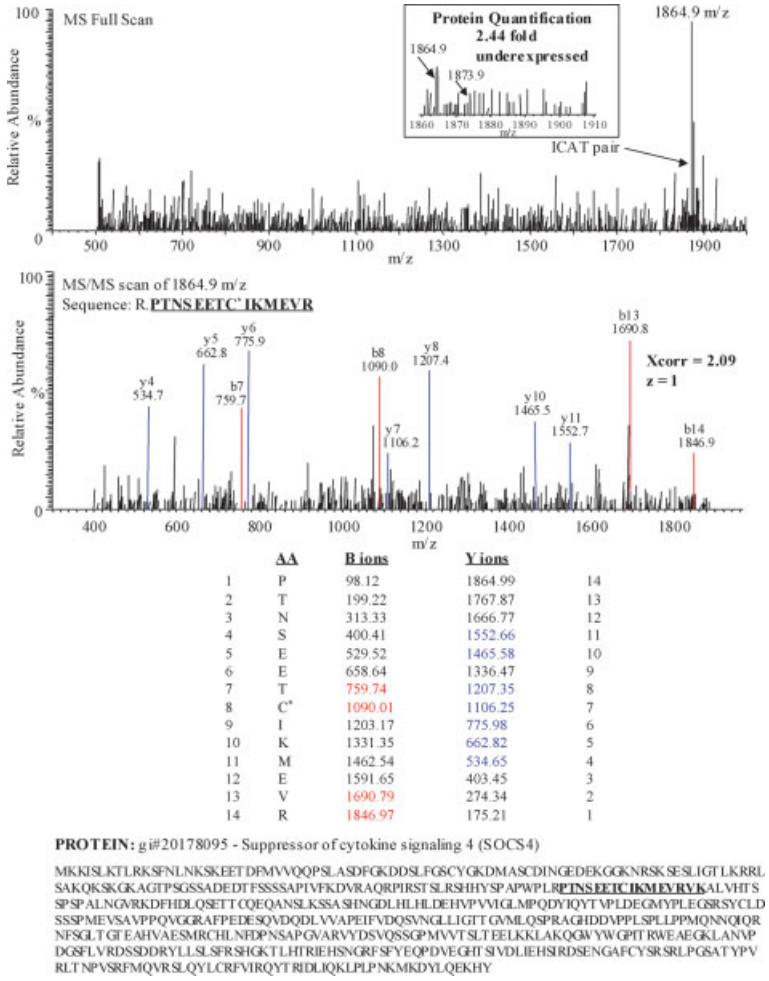

	AA	B ions	Y ions	
1	P	98.12	1864.99	14
2	T	199.22	1767.87	13
3	N	313.33	1666.77	12
4	S	400.41	1552.66	11
5	E	529.52	1465.58	10
6	E	658.64	1336.47	9
7	T	759.74	1207.35	8
8	C*	1090.01	1106.25	7
9	I	1203.17	775.98	6
10	K	1331.35	662.82	5
11	M	1462.54	534.65	4
12	E	1591.65	403.45	3
13	V	1690.79	274.34	2
14	R	1846.97	175.21	1

PROTEIN: gi#20178095 - Suppressor of cytokine signaling 4 (SOCS4)

MKKISLKTLRKSFNLNKSKEETDFMVVQQPSLASDFGKDDSLFGSCYGKDMASCDINGEDEKGGKNRSKSESLIGTLKRRL
SAKQKSKGKAGTPSGSSADEDTFSSSSAPIVFKDVRAQRPIRSTSLRSHHYSPAPWPLRPTNSEETCIKMEVRVKALVHTS
SPSPALNGVRKDFHDLQSETTCQEQANSLKSSASHNGDLHLHLDEHVPVVIGLMPQDYIQYTVPLDEGMYPLEQSRSYCLD
SSSPMEVSAVPPQVGGRAFPEDESQVDQDLVVAPEIFVDQSVNGLLIGTTGVMLQSPRAGHDDVPPLSPLLPPMQNNQIQR
NFSGLTGTEAHVAESMRCHLNFDPNSAPGVARVYDSVQSSGPMVVTSLTEELKKLAKQGWYWGPITRWEAEGKLANVP
DGSFLVRDSSDDRYLLSLSFRSHGKTLHTRIEHSNGRFSFYEQPDVEGHTSIVDLIEHSIRDSENGAFCYSRSRLPGSATYPV
RLTNPVSRFMQVRSLQYLCRFVIRQYTRIDLIQKLPLPNKMKDYLQEKHY

Figure 4. Identification of SOCS4 by LC-MS/MS. MS full scan and data-dependent MS/MS scan showing sequencing of the cICAT tryptic peptide R.PTNSEETC*IKMEVR, which identified SOCS4 as underexpressed 2.44-fold. Peptide sequencing is indicated by matching *b*-ion (red) and *y*-ion (blue) fragments.

a protein enzyme USP2, which was identified as being involved in ubiquitin-mediated proteolysis, MAPK signaling, and PPAR signaling.

Analysis of proteins further implicated those involved in JAK/STAT (underexpressed: IL26, CBLC, and SOCS4), WNT (overexpressed: WNT10B; underexpressed: DKK2, NEMO, and RAC3), MAPK (overexpressed: IL1R1, MAP4K1, MAPK14, RASA3, and Rap guanine nucleotide exchange factor (RAPGEF6); underexpressed: NEMO and RAC3), NF-κB (underexpressed: TNFRSF11B and NEMO), and TGFβ (underexpressed: RPS6KB1 and SMAD5) pathways.

3.6 Immunoblot validation of differentially expressed proteins

We selected eight differentially expressed proteins identified by cICAT-LC-MS/MS to validate changes in expression by immunoblot. Importantly, relative differences between cICAT and immunoblot were within 50% of each other. Immunoblot analysis demonstrated that USP9, ras GTPase-activating protein 3 (GAP1), PCLN1, and STCN were over-expressed in GA-treated cells relative to control by 5.6-, 2.8-, 2.6-, and 2.1-fold (cICAT), respectively. Proteins that were underexpressed in GA-treated cells including tankyrase, SOCS4, IKKκ (NEMO), and OPG were also confirmed by immunoblot analysis and were reduced by 4.2-, 2.4-, 2.4-, and 1.8-fold (cICAT), respectively, relative to control. Figure 6 illustrates the respective overexpressed proteins (left panels) and underexpressed proteins (right panels) with corresponding cICAT and densitometry ratios.

4 Discussion

ALK-positive ALCLs are most commonly associated with the t(2;5)(p23;q35) chromosomal aberration, resulting in expression of the chimeric NPM-ALK oncoprotein [1–3]. Survival of ALK-positive ALCL cells is mediated by the activation of signaling pathways [7–12] that inhibit apoptosis and promote cell proliferation [13]. Vital to the survival of these cells is the function of the chaperone protein Hsp90, which enhances the stability of the NPM-ALK protein [14, 15].

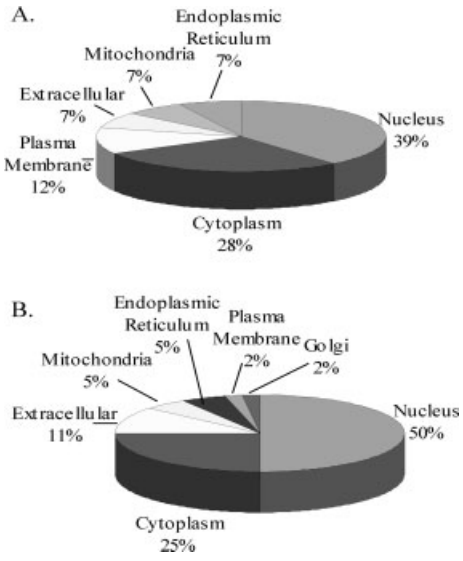

Figure 5. Cellular localization of proteins identified by MS/MS in upregulated (A) and downregulated (B) proteins. Protein from control and cells exposed to 10 μM GA were harvested after 12 h incubation and cICAT-labeled followed by LC-MS/MS analysis. Peptides were searched against the NCBI database for localization. Proteins overexpressed (A) or underexpressed (B) were categorized by cellular localization.

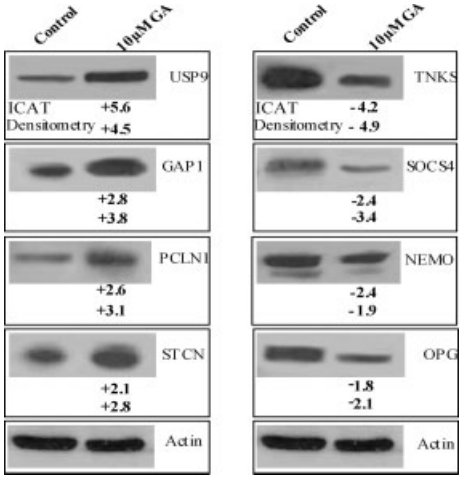

Figure 6. Immunoblot validation of differentially expressed proteins as identified by LC-MS/MS. Total cell lysate was extracted from control and GA-treated cells after 12 h and proteins separated by SDS-PAGE. Immunoblots were probed with anti-USP9 (1:1000), anti-GAP1 (1:300), anti-PCLN (1:300), anti-STCN (1:300), anti-tankyrase (1:1000), anti-SOCS-4 (1:1000), anti-NEMO (1:1000), anti-OPG (1:500), and anti-actin (1:500). Immunoblots were then incubated at room temperature for 1 h followed by probing with respective HRP-conjugated secondary antibodies and visualized by chemiluminescence. The left panels depict the overexpressed proteins as identified by LC-MS/MS in control and cells exposed to 10 μM GA. The right panels depict the underexpressed proteins as identified in the same samples. Both cICAT- and densitometry fold-change is listed below the 10 μM GA lanes. Actin served as a loading control.

Hsp90 assists in the functional maturation of a diverse group of proteins, particularly those involved in cancer-related signaling [16]. GA binds to the N-terminus ATP-binding domain of Hsp90, thereby preventing Hsp90 from performing its chaperone duties [27]. Inhibition of Hsp90 by ansamycins reduces the expression levels of its client proteins by subjecting them to ubiquitin-mediated proteasomal degradation [14, 28]. GA and its analog, 17-AAG, have been shown to reduce the expression of NPM-ALK and result in subsequent cellular apoptosis [14, 15]. However, the comprehensive proteomic changes induced by the drug are currently unknown. The results of our quantitative proteomic study demonstrate that the effects of GA on ALK-positive ALCL cells are diverse and affect proteins involved in cell signaling, DNA metabolism, protein metabolism, cell growth, and transport.

In this study, we demonstrate that the NPM-ALK-positive ALCL cell line, SU-DHL-1, is sensitive to GA inhibition of Hsp90. The display of both increased caspase-3 activity (Fig. 2D) and cleavage of PARP (Fig. 3) indicate that Hsp90 inhibition by GA induces the mitochondria-mediated apoptotic pathway, in line with other studies using GA in a variety of cell lines [29–32]. Furthermore, GA treatment resulted in the downregulation of both the native NPM-ALK and phospho-NPM-ALK (Fig. 3), in agreement with previous studies using 17-AAG in ALK-positive ALCL cells [14, 15]. These results reinforce the critical role of NPM-ALK in the survival of these cells [14, 15]. We further showed that the expression of Hsp90 itself did not change in response to GA treatment (Fig. 3), suggesting that GA does not inhibit expression of Hsp90 [33].

Cell cycle analysis revealed that GA induced G_2/M cell cycle arrest (Fig. 2B). While this observation contradicts other studies that report G_1 arrest in cells exposed to 17-AAG [14, 15], GA has been shown to induce G_2/M arrest in erythroleukemic cells through inhibition of Cdc2 and induction of $p27^{Kip1}$ [34] and other G_2/M regulators [17]. The induction of $p27^{Kip1}$ but not $p21^{Cip1}$ (Fig. 3) observed in our studies is consistent with G_2/M cell cycle arrest.

Analysis of the proteome of GA-treated cells demonstrated that numerous proteins that perform diverse cellular functions are affected by Hsp90 inhibition (Table 1). Proteins known to be involved in signaling pathways important for survival of ALK-positive ALCL cells include PI3K/AKT [8, 9], JAK/STAT [10, 11], and PLCγ [7]. Our quantitative proteomic analysis revealed differential expression of proteins belonging to multiple signaling pathways including those in the MAPK (overexpressed: MAP4K1, RASA3, RAPGEF6, MAPK14, and IL1R1; underexpressed: NEMO and RAC3), JAK/STAT (underexpressed: IL26, CBLC, and SOCS4), WNT (overexpressed: WNT10B; underexpressed: RAC3, NEMO, and DKK2), NF-κB (overexpressed: IL1R1; underexpressed: NEMO and TNFRSF11B), and TGFβ (underexpressed: RPS6KB1 and SMAD5) pathways. Because of the roles of these pathways in survival signaling, we were surprised to identify 41% overexpressed proteins. However, because

samples were analyzed after 12 h drug exposure, these results may be indicative of secondary and tertiary effects of the drug on MAPK signaling. For example, MAP4K1 has been reported to influence FAS-mediated apoptosis and caspase-3-mediated cleavage of MAP4K1 at Asp385 converting MAP4K1 from an activator of the transcription factor NF-κB into an NF-κB inhibitor, thus favoring apoptosis [35, 36].

The role of Hsp90 as a molecular chaperone involved in the folding of protein kinases has been well described [18, 37, 38]. Our study also showed that GA treatment resulted in decreased expression of many protein kinases (PTK2B, RPS6KB1, and MAK), including serine/threonine kinases (RPS6KB1 and MAK), and tyrosine kinase (PTK2B) and NPM-ALK. Whether these protein kinases are downstream targets of NPM-ALK and/or client proteins of Hsp90 remains to be determined.

Several Hsp90 client proteins and interactors were found to be differentially expressed by quantitative proteomics and validated by immunoblot analysis, including NPM-ALK, STIP1 [39], NEMO [40], MAK [41], and MCPH1 [42]. Importantly, all of the identified Hsp90 clients and interactors were underexpressed in response to GA, which provides further validation of our results. Moreover, these data suggest that many of the diverse proteins whose expression changed in response to GA may be due to the reduced expression of Hsp90 clients and interactors other than, or in addition to, NPM-ALK. For example, STIP1 has been shown to mediate the association of the Hsp70-client protein complex with Hsp90 [39]. Moreover, the reduced expression of STIP1 may be indicative of incapacitated Hsp90, and could serve as a surrogate marker of disease states in which Hsp90 is overexpressed.

GA inhibits signal transduction by inducing ubiquitination and proteasomal degradation of proteins chaperoned by Hsp90 [16, 20, 43]. Proteins associated with ubiquitin-mediated proteasomal degradation machinery were differentially expressed (overexpressed: PDC, CBLC, PSMD9, USP9X, and PSMD7; underexpressed: PSMD2, CAPN5, and VCIP135). Interestingly, two of the overexpressed proteins (PSMD9 and PSMD7) are non-ATPase members of the 26S proteasome. PDC functions in preventing proteins from being degraded and associates with a subunit of the 26S proteasome/19S regulatory complex [44, 45] suggesting that Hsp90 may regulate the expression of components of the proteasome.

In summary, our studies illustrate the diverse proteins whose expression is changed due to GA inhibition of Hsp90. Importantly, we identified proteins of both known and previously unreported signaling pathways downregulated in response to GA-treatment. We also identified downregulated Hsp90 client proteins and direct interactors as well as upregulation of proteins involved in the 26S proteasome. Our studies illustrate the utility of a proteomics-based approach in the identification and relative quantification of proteins and signaling pathways involved in cancer pathogenesis and the potential for exploitation of new knowledge thereby obtained in approaches to the specifically targeting deranged signaling pathways.

This work was supported by the ARUP Institute for Clinical and Experimental Pathology. Supported in part by the ARUP Institute for Clinical and Experimental Pathology and the Children's Oncology Group Translated Research Award to M. S. L.

5 References

[1] Bullrich, F., Morris, S. W., Hummel, M., Pileri, S. *et al.*, *Cancer Res.* 1994, *54*, 2873–2877.

[2] Morris, S. W., Kirstein, M. N., Valentine, M. B., Dittmer, K. G. *et al.*, *Science* 1994, *263*, 1281–1284.

[3] Shiota, M., Nakamura, S., Ichinohasama, R., Abe, M. *et al.*, *Blood* 1995, *86*, 1954–1960.

[4] Borer, R. A., Lehner, C. F., Eppenberger, H. M., Nigg, E. A., *Cell* 1989, *56*, 379–390.

[5] Bischof, D., Pulford, K., Mason, D. Y., Morris, S. W., *Mol. Cell Biol.* 1997, *17*, 2312–2325.

[6] Morris, S. W., Naeve, C., Mathew, P., James, P. L. *et al.*, *Oncogene* 1997, *14*, 2175–2188.

[7] Bai, R. Y., Dieter, P., Peschel, C., Morris, S. W., Duyster, J., *Mol. Cell. Biol.* 1998, *18*, 6951–6961.

[8] Slupianek, A., Skorski, T., *Exp. Hematol.* 2004, *32*, 1265–1271.

[9] Bai, R. Y., Ouyang, T., Miething, C., Morris, S. W. *et al.*, *Blood* 2000, *96*, 4319–4327.

[10] Amin, H. M., Medeiros, L. J., Ma, Y., Feretzaki, M. *et al.*, *Oncogene* 2003, *22*, 5399–5407.

[11] Zamo, A., Chiarle, R., Piva, R., Howes, J. *et al.*, *Oncogene* 2002, *21*, 1038–1047.

[12] Cussac, D., Greenland, C., Roche, S., Bai, R. Y. *et al.*, *Blood* 2004, *103*, 1464–1471.

[13] Hunter, T., *Cell* 1997, *88*, 333–346.

[14] Bonvini, P., Dalla Rosa, H., Vignes, N., Rosolen, A., *Cancer Res.* 2004, *64*, 3256–3264.

[15] Bonvini, P., Gastaldi, T., Falini, B., Rosolen, A., *Cancer Res.* 2002, *62*, 1559–1566.

[16] Neckers, L., Schulte, T. W., Mimnaugh, E., *Invest New Drugs* 1999, *17*, 361–373.

[17] Picard, D., *Cell Mol. Life Sci.* 2002, *59*, 1640–1648.

[18] Galigniana, M. D., Scruggs, J. L., Herrington, J., Welsh, M. J. *et al.*, *Mol. Endocrinol.* 1998, *12*, 1903–1913.

[19] Caplan, A. J., Jackson, S., Smith, D., *EMBO Rep.* 2003, *4*, 126–130.

[20] Neckers, L., Mimnaugh, E., Schulte, T. W., *Drug Resist. Updat.* 1999, *2*, 165–172.

[21] Lin, Z., Crockett, D. K., Jenson, S. D., Lim, M. S., Elenitoba-Johnson, K. S., *Mol. Cell Proteomics* 2004, *3*, 820–833.

[22] Lim, M. S., Elenitoba-Johnson, K. S., *Lab. Invest* 2004, *84*, 1227–1244.

[23] Marchal, J. A., Boulaiz, H., Suarez, I., Saniger, E. *et al.*, *Invest New Drugs* 2004, *22*, 379–389.

[24] Piccotti, J. R., LaGattuta, M. S., Knight, S. A., Gonzales, A. J., Bleavins, M. R., *Drug Chem. Toxicol.* 2005, *28*, 117–133.

[25] Gygi, S. P., Rist, B., Gerber, S. A., Turecek, F. *et al.*, *Nat. Biotechnol.* 1999, *17*, 994–999.

[26] Peng, J., Elias, J. E., Thoreen, C. C., Licklider, L. J., Gygi, S. P., *J. Proteome Res.* 2003, *2*, 43–50.

[27] Grenert, J. P., Sullivan, W. P., Fadden, P., Haystead, T. A. *et al.*, *J. Biol. Chem.* 1997, *272*, 23843–23850.

[28] Takimoto, C. H., Diggikar, S., *Hematol. Oncol. Clin. North Am.* 2002, *16*, 1269–1285.

[29] Castro, J. E., Prada, C. E., Loria, O., Kamal, A. *et al.*, *Blood* 2005, *7*, 2506–2512.

[30] Yun, B. G., Matts, R. L., *Exp. Cell. Res.* 2005, *307*, 212–223.

[31] Kaarniranta, K., Ryhanen, T., Karjalainen, H. M., Lammi, M. J. *et al.*, *Neurosci. Lett.* 2005, *382*, 185–190.

[32] Nomura, M., Nomura, N., Newcomb, E. W., Lukyanov, Y. *et al.*, *J. Cell Physiol.* 2004, *201*, 374–384.

[33] Sittler, A., Lurz, R., Lueder, G., Priller, J. *et al.*, *Hum. Mol. Genet.* 2001, *10*, 1307–1315.

[34] Kim, H. R., Lee, C. H., Choi, Y. H., Kang, H. S., Kim, H. D., *IUBMB Life* 1999, *48*, 425–428.

[35] Chen, Y. R., Meyer, C. F., Ahmed, B., Yao, Z., Tan, T. H., *Oncogene* 1999, *18*, 7370–7377.

[36] Arnold, R., Liou, J., Drexler, H. C., Weiss, A., Kiefer, F., *J. Biol. Chem.* 2001, *276*, 14675–14684.

[37] Kanelakis, K. C., Pratt, W. B., *Methods Enzymol.* 2003, *364*, 159–173.

[38] Morishima, Y., Kanelakis, K. C., Murphy, P. J., Lowe, E. R. *et al.*, *J. Biol. Chem.* 2003, *278*, 48754–48763.

[39] Odunuga, O. O., Longshaw, V. M., Blatch, G. L., *Bioessays* 2004, *26*, 1058–1068.

[40] Chen, G., Cao, P., Goeddel, D. V., *Mol. Cell* 2002, *9*, 401–410.

[41] Miyata, Y., Nishida, E., *Mol. Cell Biol.* 2004, *24*, 4065–4074.

[42] McCarty, M. F., *Integr. Cancer Ther.* 2004, *3*, 349–380.

[43] Vasilevskaya, I. A., O'Dwyer, P. J., *Cancer Res.* 1999, *59*, 3935–3940.

[44] Barhite, S., Thibault, C., Miles, M. F., *Biochim. Biophys. Acta* 1998, *1402*, 95–101.

[45] Flanary, P. L., DiBello, P. R., Estrada, P., Dohlman, H. G., *J. Biol. Chem.* 2000, *275*, 18462–18469.

